Effects of Subretinal Electrical Stimulation in Mer-KO Mice

Julie A. Mocko,[1] *Moon Kim,*[1] *Amanda E. Faulkner,*[1] *Yang Cao,*[1] *Vincent T. Ciavatta,*[1] *and Machelle T. Pardue*[1,2]

Purpose. Subretinal electrical stimulation (SES) from microphotodiode arrays protects photoreceptors in the RCS rat model of retinitis pigmentosa. The authors examined whether *mer*^{kd} mice, which share a *Mertk* mutation with RCS rats, showed similar neuroprotective effects from SES.

Methods. *Mer*^{kd} mice were implanted with a microphotodiode array at postnatal day (P) 14. Weekly electroretinograms (ERGs) followed by retinal histology at week 4 were compared with those of age-matched controls. RT-PCR for fibroblast growth factor beta (*Fgf2*), ciliary nerve trophic factor (*Cntf*), glial-derived neurotrophic factor (*Gdnf*), insulin growth factor 1 (*Igf1*), and glial fibrillary acidic protein (*Gfap*) was performed on retinas at 1 week after surgery. Rates of degeneration using ERG parameters were compared between *mer*^{kd} mice and RCS rats from P28 to P42.

Results. SES-treated *mer*^{kd} mice showed no differences in ERG a- and b-wave amplitudes or photoreceptor numbers compared with controls. However, the expression of *Fgf2* and *Cntf* was greater (6.5 $\pm$ 1.9- and 2.5 $\pm$ 0.5-fold, respectively; $P < 0.02$) in SES-treated *mer*^{kd} retinas. Rates of degeneration were faster for dark-adapted maximal b-wave, log σ, and oscillatory potentials in *mer*^{kd} mice than in RCS rats.

Conclusions. Although SES upregulated *Fgf2* in *mer*^{kd} retinas, as reported previously for RCS retinas, this was not accompanied by neuroprotection of photoreceptors. Comparisons of ERG responses from *mer*^{kd} mice and RCS rats across different ages showed inner retinal dysfunction in *mer*^{kd} mice but not in RCS rats. This inner retinal dysfunction and the faster rate of degeneration in *mer*^{kd} mice may produce a retinal environment that is not responsive to neuroprotection from SES. (*Invest Ophthalmol Vis Sci.* 2011;52:4223–4230) DOI:10.1167/iovs.10-6750

Retinal degenerative diseases, such as retinitis pigmentosa (RP) and age-related macular degeneration (AMD), are major causes of blindness caused by progressive photoreceptor cell death. Many of these diseases share abnormalities in the retinal pigment epithelium (RPE),[1–7] a tissue critical for maintaining photoreceptor outer segment (OS) integrity and function and, thus, critical for normal vision. The RPE mediates the visual cycle by converting all-*trans*-retinal into its photoreactive *cis*-isomer and participates in the circadian phagocytosis of shed OS discs. The receptor tyrosine kinase Mertk is necessary for triggering the ingestion of shed OS discs in the RPE,[8] and mutations in the gene encoding Mertk lead to an accumulation of cellular debris, the breakdown of OS, and the eventual death of photoreceptors.[9–13] Mutations in this gene have been implicated in RP.[7]

The Royal College of Surgeon (RCS) rat is a commonly studied animal model of retinal degeneration[14,15] and is known to have a spontaneously occurring null mutation of the *Mertk* gene.[16] A functional knockout mouse, called the *mer*^{kd} mouse, with a truncated cytoplasmic tail of the Mer receptor tyrosine kinase[17] displays a retinal phenotype similar to that of the RCS rat.[13] Although both animals share a mutation in the same gene and experience retinal degeneration caused by RPE dysfunction, they are known to have differences in morphology with the progression of disease. Photoreceptor degeneration in RCS rats begins at approximately postnatal day (P) 12 and is nearly complete by P77.[12] The degeneration is also graded and preferential, with more cell loss in the inferior portion of the retina[12] and greater loss of rod photoreceptors than cones.[18] In these rats, OS debris can remain for several months after photoreceptor cell death.[13] *Mer*^{kd} mice, on the other hand, exhibit a more rapid degeneration than do RCS rats and lose OS debris and photoreceptor nuclei concomitantly.[13]

Although there is no cure for retinal degeneration, many treatments for retinal degenerative diseases are being developed, such as gene therapy,[19–21] use of neurotrophic factors,[22,23] retinal cell transplantation,[24,25] retinal prosthesis,[26–29] and electrical stimulation.[30,31] Low-level electrical stimulation is being pursued as a neuroprotective treatment of the eye using either an external (transcorneal) or a subretinal approach. Some of these studies have found benefit in retinal degeneration (Morimoto T, et al. *IOVS* 2005;46:ARVO Abstract B157),[32] retinal artery occlusion,[33] optic neuropathy,[34] and axotomized ganglion cells.[35,36] Our previous studies have shown that subretinal electrical stimulation with an implanted microphotodiode array had a neuroprotective effect in RCS rats[30] and that this effect was associated with an upregulation in fibroblast growth factor beta (*Fgf2*) expression.[37]

To address the generalized applicability of these neuroprotective treatments to the large family of mutations that cause RP and other types of photoreceptor degeneration, it is important to examine several mutant models. Equally important is the need to determine whether the phenotype of a mutation is conserved across species. In this study, using electroretinography, photoreceptor cell counts, and real-time PCR, we investigated whether subretinal electrical stimulation (SES) would have the same neuroprotective effect and growth factor expression change in *mer*^{kd} mice as it does in RCS rats. We also

From the [1]Rehabilitation Research and Development Service, Atlanta Department of Veterans Affairs, Decatur, Georgia; and the [2]Department of Ophthalmology, Emory University, Atlanta, Georgia.

Supported by the Rehabilitation Research and Development Service, Atlanta Department of Veterans Affairs; Research to Prevent Blindness; and a National Institutes of Health core grant (Department of Ophthalmology).

Submitted for publication October 19, 2010; revised February 21, 2011; accepted March 4, 2011.

Disclosure: **J.A. Mocko**, None; **M. Kim**, None; **A.E. Faulkner**, None; **Y. Cao**, None; **V.T. Ciavatta**, None; **M.T. Pardue**, None

Corresponding author: Machelle T. Pardue, Rehabilitation Research and Development Service, Atlanta Department of Veterans Affairs, Atlanta VA Medical Center, 1670 Clairmont Road, Decatur, GA 30033; mpardue@emory.edu.

compared the rates of degeneration in the RCS rats and *mer*^{kd} mice to determine whether there are phenotypic differences in retinal function over the course of the degeneration between the two animal models.

Methods

Animals and Experimental Design

Mer^{kd} mice[13] and dystrophic RCS rats were obtained from Douglas Vollrath (Stanford University) and Matthew LaVail (University of California at San Francisco), respectively, and were maintained as homozygous breeding colonies at the Atlanta VA Medical Center. Animals were housed on a 12-hour light (fluorescent lighting, 25–200 lux)/12-hour dark cycle and were provided food and water ad libitum. SES was provided by an implanted active microphotodiode array (MPA) as previously described.[38,39] Eighteen *mer*^{kd} mice underwent monocular implantation surgery[40] at P14, near the beginning of the retinal degeneration; 13 *mer*^{kd} mice served as unoperated controls. Of those mice, eight implanted and four control animals had ERG recordings 1 week after surgery and were killed 2 days later for gene expression analysis. Weekly ERG recordings were performed on the remaining mice for 4 weeks, beginning 1 week after surgery (P21, P28, P35, P42). Mice were immediately killed after the last ERG, and eyes were enucleated for histologic processing and photoreceptor cell counts.

For data analysis, the mouse eyes were divided into active (implanted eye), opposite (contralateral eye), and control (eyes of naive unoperated control animals) groups. For comparison of retinal function between *mer*^{kd} mice and RCS rats, a group of unoperated mice ($n = 10$) and rats ($n = 10$) was also studied. Weekly ERGs were recorded, and three test ages were analyzed (P28, P35, P42).

All animal procedures were approved by the Institutional Animal Care and Use Committee of the Atlanta Veterans Administration and were in full compliance with the standards of the ARVO Statement for the Use of Animals in Ophthalmic and Visual Research.

Subretinal Implant Description

The active MPA consisted of a silicon disc (25-μm thick, 0.5-mm diameter) covered by 1200 microphotodiodes (9×9 μm) on one side and coated with iridium oxide on the other side, as previously described.[38,39] These diodes are sensitive to incident light ranging in wavelength from 500 to 1100 nm.[39] Most of the wavelengths in the animals' environment fell between 500 and 650 nm, with a mean irradiance of 0.1 to 10 μW/cm^2. Within this range, the MPA responds at ~0.3 amp/W, thus producing currents estimated to range from several nA/cm^2 to 1 μA/cm^2.[30] The electrical activity of the implant was confirmed in each animal during ERG recordings when the implant spike appeared in the ERG trace immediately after flash onset at the brightest flash intensities (Supplementary Fig. S1, http://www.iovs.org/lookup/suppl/doi:10.1167/iovs.10-6750/-/DCSupplemental).

Implantation Surgery

MPAs were monocularly implanted into the subretinal space of 18 *mer*^{kd} mice as previously described.[40] Briefly, the mice were anesthetized with a mixture of ketamine (80 mg/kg) and xylazine (16 mg/kg) and were placed in a sterile surgical area on a water-filled heating pad to maintain body temperature. A traction suture was placed in the superior conjunctiva at the edge of the limbus to pull the eye downward and to expose the superior portion of the conjunctiva. The mouse eye at P14 is approximately 2.5 mm in diameter. A small incision was made in the globe through the sclera into the vitreous,

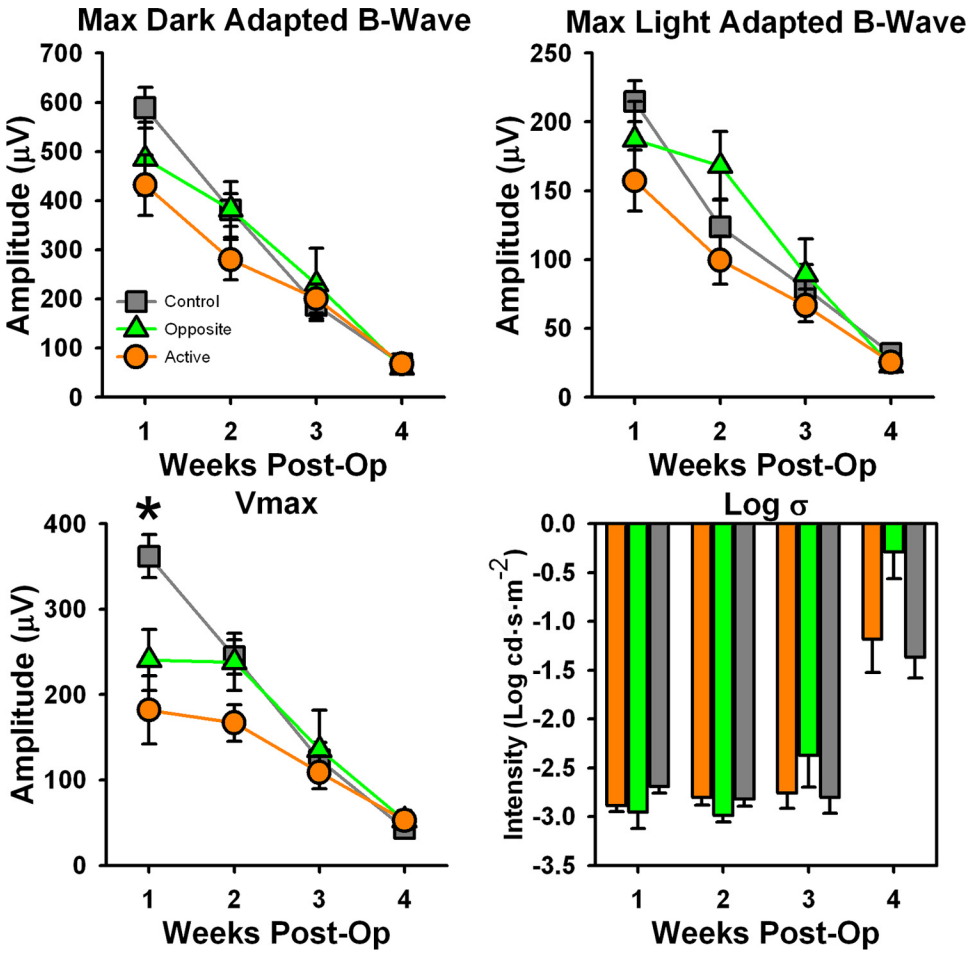

Figure 1. Measured (**A**, **B**) and derived (**C**, **D**) ERG parameters. Measured ERG parameters, (**A**) maximal dark adapted b-wave amplitude, and (**B**) maximal light adapted b-wave amplitude showed no differences between groups at any time point. (**C**) V_{max}, derived from Naka-Rushton fit to b-wave amplitude, was significantly higher in control eyes (*gray squares*) than in active eyes (*orange circles*) 1 week after surgery. (**D**) *Log* σ, a postreceptoral sensitivity measure derived from Naka-Rushton fit, did not differ between groups for any time point. $^*P < 0.001$.

and a drop of 0.9% sodium chloride was placed at the incision site to facilitate creation of a local retinal detachment. After 5 minutes, the implant was gently inserted between the retina and the RPE, and the position was confirmed by fundus examination.

Electroretinography

ERGs were recorded under both dark- and light-adapted conditions, as previously described.[30,37] Animals were dark adapted overnight or for at least 4 hours andFig. 2 were prepared under dim red illumination. After anesthesia with ketamine (mice, 80 mg/kg; rats, 60 mg/kg) and xylazine (mice, 16 mg/kg; rats, 7.5 mg/kg), the cornea was anesthetized (0.5% tetracaine) and pupils were dilated (1.0% cyclopentolate, 1.0% tropicamide). Body temperature was maintained at 37°C on a homeothermic heating pad. Responses were recorded binocularly with a nylon fiber embedded with silver particles laid across the corneal surface[41] and wetted with 1% methylcellulose to maintain corneal moisture. Platinum needle electrodes serving as reference and ground were placed in the cheeks and tail, respectively. Under dark-adapted conditions, a series of full-field flash stimuli ranging from −3.4 to 2.1 log cd · s/m^2 were presented to both eyes by a Ganzfeld dome. With increasing intensity, the interstimulus interval increased from 2 to 70 seconds, and 3 to 10 flashes were averaged to generate a waveform for each flash intensity. Eyes were then light adapted for 10 minutes (30 cd · m^{-2} background), and a series of cone-isolating stimuli (−0.8 to 1.9 log cd · s/m^2) was presented at 2.1 Hz in the presence of the adapting field. Each photopic waveform was an average of 25 flashes. Responses were filtered (1–1500 Hz) and stored on a commercial ERG system (UTAS 3000; LKC Technologies, Gaithersburg, MD).

Details about the ERG analysis can be found in the Supplementary Methods (http://www.iovs.org/lookup/suppl/doi:10.1167/iovs.10-6750/-/DCSupplemental). Briefly, ERG waveform measurements consisted of b-wave amplitudes for both dark- and light-adapted conditions. The Naka-Ruston stimulus-response function was fitted to the dark-adapted b-wave amplitude to assess postreceptoral function and the activity of the rod bipolar cells.[42–45] Dark-adapted oscillatory potentials (OPs) were extracted from raw traces using a fifth-order Butterworth filter[46] (MatLab; The MathWorks, Natick, MA) with bandpass 65 to 300 Hz for mice[46] and 65 to 235 Hz for rats.[47,48] The amplitudes and implicit times of individual OP1 through OP6 were determined, as were summed OP amplitude and implicit time.[48] A discrete Fourier transform was also used to analyze the OPs in the frequency domain.[49]

Rates of degeneration, defined as the loss of amplitude (μV) or sensitivity (log cd · s/m^2) per week, for the different ERG parameters were also examined. Because of the small number of test ages, the rate of degeneration was calculated as the slope of a linear fit between the measures at postoperative week 1 and 4. To determine the effect of SES on the progression of disease, the rates of degeneration between active and opposite eyes were compared. For a comparison of rates of degeneration between naive control *mer^{kd}* mice and RCS rats, rates of degeneration were calculated as the slope of a linear fit for matching ages between P28 and P42.

Histologic Examination

Four weeks after surgery, animals (10 implanted, 9 control) were euthanized by an overdose of anesthesia. Eyes were prepared and analyzed as previously described.[30] Briefly, eyes were enucleated and fixed overnight in 2% paraformaldehyde and 2.5% glutaraldehyde, after

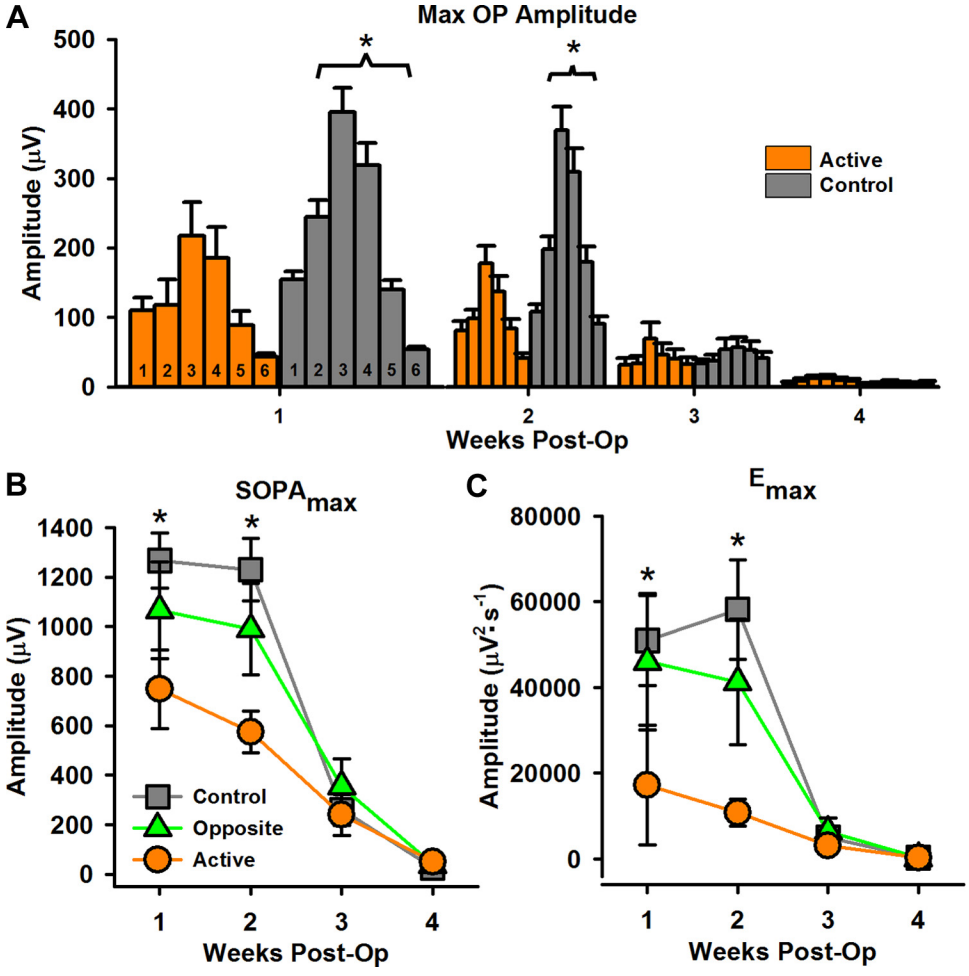

FIGURE 2. OP parameters. (**A**) Average maximal OP amplitude for all OPs 1–6 across time (1–4 weeks after surgery) for active (*orange bars*) and control (*gray bars*) groups. Numbers at the bottom of each bar indicate the OP number. At weeks 1 and 2 after surgery, control eyes had significantly larger maximal OP amplitudes for OP2–6 than active eyes. Responses from opposite eyes did not differ from those of control eyes. (**B**, **C**) Average maximal summed OP amplitude ($SOPA_{max}$) and maximal OP energy (E_{max}). Control eyes (*gray squares*) had significantly larger responses than active eyes (*orange circles*) at weeks 1 and 2 after surgery for both parameters. $^*P \leq 0.04$.

which the cornea and lens were removed. The posterior eyecup was dehydrated with a graded series of alcohols and embedded in resin (Embed 812/DER 736; Electron Microscopy Sciences, Fort Washington, PA). Vertical sections (0.5 μm) were cut through both the retina and the implant and were stained with toluidine blue. Photoreceptor nuclei were counted using an image analysis computer program (ImagePro Plus; Media Cybernetics, Inc., Bethesda, MD) in four 0.5-mm regions of the retina on either side of the optic nerve.

Growth Factor Expression Analysis

Two days after the first ERG (P23), animals (8 implanted, 4 control) were euthanatized with an overdose of pentobarbital. Tissue preparation and growth factor expression were performed as previously described.[37] Briefly, eyes were enucleated, the cornea and lens were removed, and a 1.8-mm-diameter portion of the retina over the implant (or an equivalent location in nonimplanted eyes) was harvested.

Total mRNA was recovered (RNeasy Micro kit with DNase Treatment; Qiagen, Valencia, CA) according to the manufacturer's instructions. mRNA (100 ng) was converted to cDNA (Quantitect Reverse Transcriptase; Qiagen). The cDNA was diluted 20-fold, and 5 μL diluted cDNA was used in real-time PCR reactions with 100 nM (*Gdnf*) or 200 nM (*Fgf2*, *Cntf, Igf-1, Gfap,* and 18S) each forward and reverse primer (see Supplementary Table S1, http://www.iovs.org/lookup/suppl/doi:10.1167/iovs.10-6750/-/DCSupplemental). Samples were run in triplicate, and the average Ct was calculated. With 18S as an internal standard, relative growth factor expression was calculated from the average PCR cycle thresholds using the $2^{-\Delta\Delta Ct}$ method.[50] The expression ratio (treated eye/opposite eye) was computed to minimize between-animal variability in gene expression.

Statistical Analysis

For intensity series data (a-wave, b-wave, OP amplitudes, and implicit times) and ERG parameters (maximal dark- and light-adapted b-wave, V_{max}, *log* σ, $OP1_{max}$-$OP6_{max}$, $SOPA_{max}$, and E_{max}), statistical comparisons were made with two-way repeated-measures ANOVA. Rates of degeneration were compared with a two-tailed paired Student's *t*-test for mer^{kd} active and opposite eyes and with an unpaired Student's *t*-test for species. Post hoc comparisons were performed between groups when appropriate. Photoreceptor cell counts across retinal locations were compared using two-way repeated-measures ANOVA. Gene expression in the different treatment groups was analyzed using one-way ANOVA. The significance level for all tests (α) was $P < 0.05$. All statistical analyses were made using statistical software (SigmaStat 3.5; Systat Software, Inc., Point Richmond, CA). All graphs include ±SEM.

Results

Electroretinographic Assessment of Mer^{kd} Retinal Function

Mer^{kd} mice in all groups showed a rapid decline of function with age. Representative dark-adapted ERG waveforms elicited by the brightest flash intensity (2.1 log cd · s/m^2) from active, opposite, and control eyes for all 4 weeks of follow-up are shown in Figure S1. At P35 (week 3 after surgery), mer^{kd} mice exhibited a negative ERG with a prominent slow negative potential interfering with the a-wave, and by P42 (week 4 after surgery) the b-wave was barely measurable in any group. These findings are in agreement with previous reports by Duncan et al.[13]

At P21 (week 1 after surgery), control eyes had significantly larger a-wave ($F_{18,379} = 3.944$; $P < 0.001$) and b-wave ($F_{18,379} = 2.248$; $P = 0.003$) responses than active eyes, but this difference disappeared by the second week, and no differences between groups for amplitude were seen at any other age (see Supplementary Fig. S2, http://www.iovs.org/lookup/suppl/doi:10.1167/iovs.10-6750/-/DCSupplemental). Implicit times did not differ between the groups at any age for any measure (data not shown). V_{max} was the only postreceptoral parameter that differed between groups, with active eyes having smaller responses than control eyes at week 1 after surgery only ($F_{6151} = 4.540$; $P < 0.001$; Fig. 1). Maximal dark- and light-adapted b-wave and postreceptoral sensitivity (*log* σ) showed no differences between groups at any age (Fig. 1). There were no differences in rates of degeneration between active and opposite eyes for a- and b-wave parameters (data not shown).

All OP amplitude parameters ($OP2_{max} - OP6_{max}$; [$F_{6151} \geq 2.307$; $P \leq 0.04$], $SOPA_{max}$ [$F_{6151} = 3.626$; $P = 0.003$], and E_{max} [$F_{6150} = 2.423$; $P = 0.031$]) were significantly attenuated in active eyes at weeks 1 and 2 after surgery compared with control eyes (). Opposite eyes were not different from control eyes. By week 3 after surgery, differences between the groups disappeared. Rates of degeneration between active and opposite eyes were significantly different for maximal OP amplitudes, with active eyes having significantly lower rates of degeneration (data not shown). However, this reduction on the degeneration rate was likely a result of attenuated OP amplitudes in the active eyes 1 week after surgery.

Photoreceptor Morphology

Morphologic assessment at week 4 after surgery (P42) showed no differences between any of the mer^{kd} groups (see Supplementary Fig. S3, http://www.iovs.org/lookup/suppl/doi:10.1167/iovs.10-6750/-/DCSupplemental). Retinas of mer^{kd} mice had normal inner retinal layers but reduced outer nuclear layer thickness (3–4 layers of photoreceptor nuclei) and a debris layer in subretinal space. Photoreceptor nuclei counts were similar for all three treatment groups. Photoreceptor numbers were significantly reduced in the inferior compared with the superior retina ($F_{7143} = 7.22$; $P < 0.001$) in all mer^{kd} mice.

Growth Factor Expression

At P23, real-time PCR expression analysis showed a 6.5- and a 2.5-fold upregulation of *Fgf2* and *Cntf*, respectively, in active

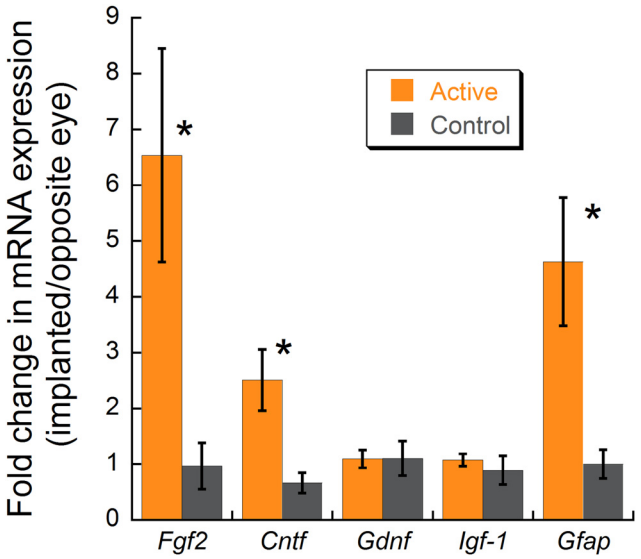

Figure 3. Growth factor RNA expression determined with RT-PCR in mer^{kd} mice after implantation. Active implanted eyes had significantly higher *Fgf2, Cntf,* and *Gfap* levels than control eyes (Student's *t*-test, $^*P < 0.02$).

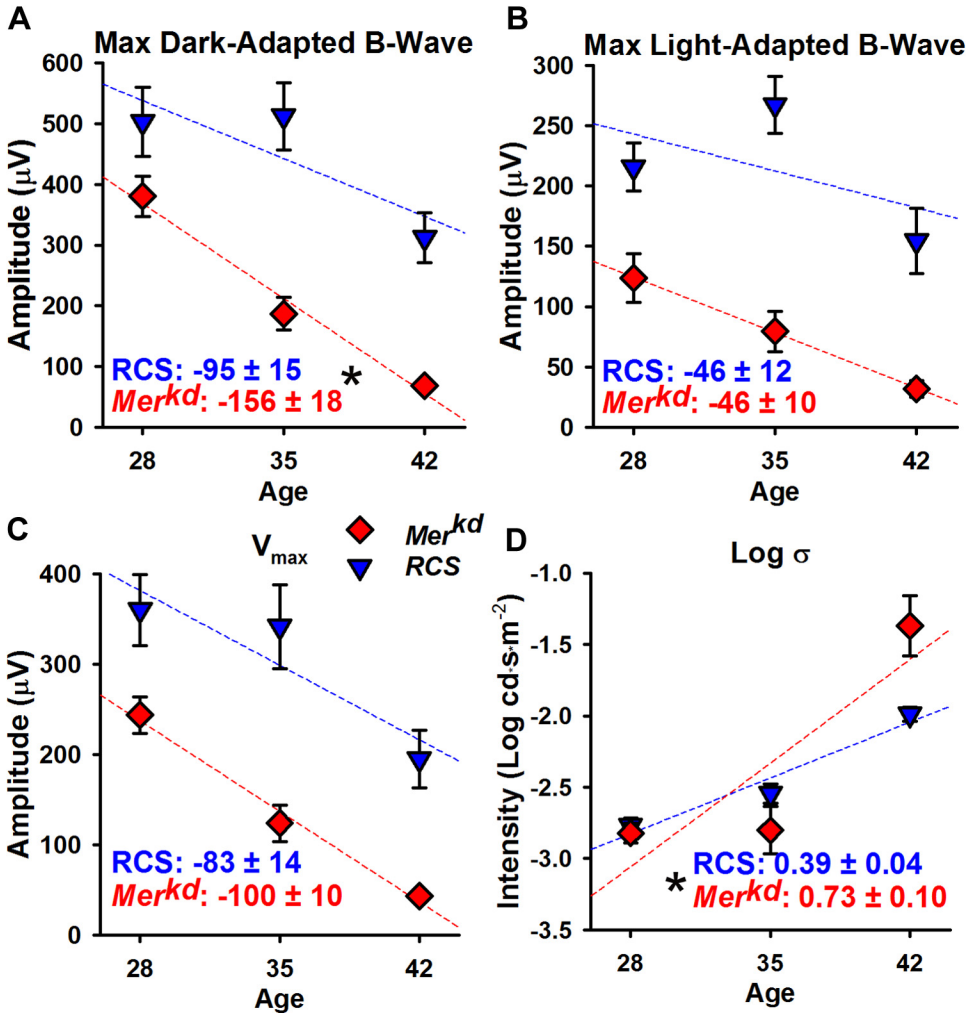

FIGURE 4. Rates of degeneration for measured (**A**, **B**) and derived (**C**, **D**) ERG parameters in *mer*^{kd} mice (*red diamonds*) and RCS rats (*blue triangles*). Rates of degeneration were calculated as a linear fit (*dashed lines*) between P28 and P42. Rates of degeneration (±SEM) are listed at the bottom of each graph. (**A**) Maximal dark-adapted b-wave degenerated significantly more quickly in *mer*^{kd} mice than in RCS rats. (**B**) Maximal light-adapted b-wave and (**C**) V_{max} were not significantly different between *mer*^{kd} mice and RCS rats. (**D**) *Log σ* degenerated more rapidly in *mer*^{kd} mice than in RCS rats. *$P \leq 0.03$.

eyes compared with control eyes (Student's *t*-test, $P < 0.02$; Fig. 3). Upregulation of *Fgf2* expression in active eyes ranged from 1- to 18-fold, with 4 of the 11 animals having expression levels above 10-fold. *Gdnf* and *Igf1* showed no significant change. *Gfap*, a marker of retinal injury, was upregulated 4.6-fold in active implanted eyes.

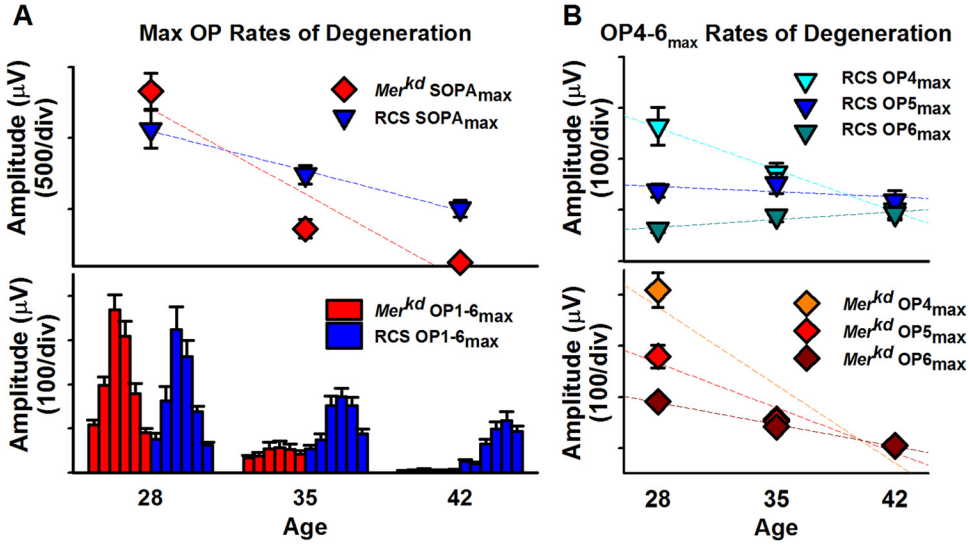

C

	$OP1_{max}$	$OP2_{max}$	$OP3_{max}$	$OP4_{max}$*	$OP5_{max}$*	$OP6_{max}$*	$SOPA_{max}$*
Merkd	-52 ± 5	-97 ± 9	-182 ± 17	-152 ± 17	-88 ± 11	-43 ± 5	-602 ± 63
RCS	-25 ± 5	-71 ± 15	-129 ± 22	-82 ± 13	-10 ± 8	-15 ± 6	-280 ± 47

FIGURE 5. Rates of degeneration in *mer*^{kd} mice (*red diamonds*) and RCS rats (*blue triangles*) for OP parameters. Rates of degeneration were calculated as a linear fit (*dashed lines*) between P28 and P42. (**A**) Rates of degeneration for $SOPA_{max}$ (*top*) and maximal OP amplitudes for $OP1–6_{max}$ (*bottom*). See Figure 2 for OP bar labels. *Mer*^{kd} mice have a more rapid rate of degeneration of $SOPA_{max}$ than RCS rats. (**B**) Rates of degeneration for late OPs ($OP4_{max}$-$OP6_{max}$) for RCS rats (*top, blue and green triangles*) and *mer*^{kd} mice (*bottom, red and orange diamonds*). Late OPs in *mer*^{kd} mice degenerated more rapidly than in RCS rats. (**C**) Rates of degeneration (±SEM) for all OPs. *$P \leq 0.003$.

Comparison of *Mer^{kd}* Mouse and RCS Rat Rates of Retinal Degeneration

To better characterize differences between the two animal models and possible sources of differences in neuroprotective effects of SES, rates of degeneration (calculated P28-P42) for naive controls of both species were compared. The first difference observed between the ERG responses of RCS rats and *mer^{kd}* mice was the absence of a negative ERG in RCS rats at any age tested. RCS rats and *mer^{kd}* mice showed similar rates of degeneration for maximal light-adapted b-wave and V_{max}, but *mer^{kd}* mice had significantly greater rates of degeneration for maximal dark-adapted b-wave (*mer^{kd}*, -156 ± 18 μV per week; RCS, -95 ± 15 μV per week; $P = 0.03$) and postreceptoral sensitivity *log* σ (*mer^{kd}*, 0.73 ± 0.10 log cd · s/m^2 per week; RCS, 0.39 ± 0.01 log cd · s/m^2 per week; $P = 0.02$; Fig. 4).

RCS rats and *mer^{kd}* mice also displayed different rates of degeneration for the OPs (Fig. 5). Although all OPs in *mer^{kd}* mice underwent rapid degeneration, those in RCS rats showed a slower decline in amplitude, with the later OPs (OP4 and OP5) declining slowly or not at all (OP6; Fig. 5B). Figure 5C lists all the rates of degeneration for the OPs of *mer^{kd}* mice and RCS rats.

Discussion

Postreceptoral Function in *Mer^{kd}* Mice after SES Treatment

Overall, the data showed no evidence of preservation or transient neuroprotection in *mer^{kd}* mouse eyes receiving SES from an MPA device. All differences between active and control groups were most likely a result of insult to the retina after surgical injury from implantation. At week 1 after surgery, active eyes had significantly attenuated V_{max} compared with controls but did not show a significant decrease in overall maximal b-wave amplitude. It is possible that rod photoreceptors were more sensitive to injury from surgery, thus resulting in attenuated rod-driven responses, whereas mixed rod-cone responses to the brightest flash intensities were unaffected, remaining at control amplitudes. The OPs were also significantly attenuated in the active implanted eyes and remained below control levels until the third week after surgery. OPs are known to be among the most sensitive of ERG components to changes in the retina; they are often affected before changes in a- or b-waves can be seen.[47,51,52] Finally, V_{max} began degenerating from the first week tested, but postreceptoral sensitivity (*log* σ) did not begin declining until the third week after surgery. The former, V_{max}, takes into account the amplification of a graded signal, which will reflect a change in the number of cells contributing to the signal. Sensitivity, on the other hand, is related to the kinetics of phototransduction. Because the *Mertk* defect does not directly affect phototransduction, it is likely photoreceptors retain functionality until structural disintegration causes cell death. If this is the case, then the functional response from the photoreceptors is appropriate for the intensity of the stimulus; there are simply fewer cells responding. This could correspond to a change in maximal amplitude (V_{max}) before a change in sensitivity (*log* σ).

Differences in Retinal Function between RCS Rats and *Mer^{kd}* Mice

Our data showed that *mer^{kd}* mice underwent more rapid retinal degeneration than RCS rats, which is consistent with other reported findings.[13] *Mer^{kd}* mice began exhibiting a negative ERG at P35, in which a significant negative wave began dominating the early portion of the response and obscuring the b-wave. By P42, there was almost no detectable response in most animals. In our previous studies, we did not observe a negative ERG in the RCS rats. In their RCS rats, however, Pinilla et al.[53] reported the appearance of a prominent negative wave interfering with a predominantly cone-driven b-wave, but not until approximately P80.

Although these negative waves have inner retinal origins, as shown through pharmacologic block by Machida et al.[54] and a double-flash protocol by Pinilla et al.,[53] the waves we observed might not have been true scotopic threshold responses (STRs). The STR, in the absence of background illumination, is seen as a slow negative potential with the lowest visual threshold of any ERG component.[55] However, in the ERGs recorded from *mer^{kd}* mice, we were able to observe a prominent negative potential coinciding with b-waves and OPs at bright flash intensities (Supplementary Fig. S1, http://www.iovs.org/lookup/suppl/doi:10.1167/iovs.10-6750/-/DCSupplemental, week 3). The OPs and STRs had nonoverlapping light intensity thresholds in the recordings of healthy eyes, thus bringing into question whether it is possible that an STR could be seen at light levels that elicit OPs and b-waves, even in degenerated retinas. To better understand the origins of this response, further studies with pharmacologic dissection of the ERG are needed at later stages of retinal degeneration in *mer^{kd}* mice.

Another difference between *mer^{kd}* mice and RCS rats was the degeneration of the OPs. Although OPs are known to originate in the inner retina, they do not all have the same generators,[56–60] and they have both rod-driven and cone-driven components.[46] The OPs in *mer^{kd}* mice were largely undetectable by P42. In RCS rats, the rates of degeneration for the early OPs were not different from the *mer^{kd}* mice, indicating that the generator of early OPs was similarly affected in both animals. However, the rates of degeneration of the later OPs were significantly slower in the RCS rats, with OP6 not showing any degeneration over the ages tested. Previous studies have shown that the proportion of cones in the RCS rat retina rises from 3% early in life[61] to 10.5% by P35.[18] Studies of rod-driven and cone-driven OPs show that cone-driven OPs are significantly slower and smaller in amplitude, contributing more to the amplitude of the later OPs in a mixed rod-cone response.[46] Taken together with other studies showing faster rod degeneration in the RCS rats,[12,15,18] these results provide further evidence that later OPs generated in response to mixed rod-cone stimuli are likely cone driven.

Differences in Effect of SES between RCS Rats and *Mer^{kd}* Mice

Our previous work has indicated that SES produces temporary preservation of photoreceptor function and morphology in RCS rats.[30] Furthermore, there appears to be a dose response to SES in that decreased frequency of ERG testing and, therefore, decreased current output from the implant eliminated the neuroprotective effect.[62] Furthermore, the neuroprotective effect is associated with the selective upregulation of FGF2.[37] Although SES showed significant neuroprotection in RCS rats,[30] SES did not produce neuroprotective effects in *mer^{kd}* mice. This could have been because *mer^{kd}* mice have a different mechanism of degeneration, resulting in more rapid degeneration than in RCS rats, as suggested. In our previous studies, comparisons of retinal function between eyes implanted with active rather than inactive devices indicated that the active implant had some positive effects, even in the initial postsurgery decline in retinal function,[30] but this was not seen as a response greater than that in controls until the retina had degenerated further and the treatment groups could separate. Thus, in *mer^{kd}* mice, the positive effects of SES may not be visible at the time points we examined in this study.

It is also possible that RCS rats are hypersensitive to neuroprotection. Previous studies have shown a neuroprotective effect in RCS rats with sham surgery that was not present in S334-ter transgenic rats given the same treatment.[63,64] In another study, RCS rats responded to neuroprotection by light stress that was not measurable in the P23H transgenic rats.[65] In our studies with normal animal models, subretinal implants caused a local photoreceptor degeneration in the area overlaying the implant,[66,67] but RCS rats implanted with the device showed preservation of photoreceptors both over the implant and in more distal areas.[30] Further studies of an animal model with a slower rate of retinal degeneration, similar to that of RCS rats and caused by an RPE defect, would be needed to determine whether neuroprotection by subretinal electrical stimulation is a feature unique to RCS rats. The ideal rat model would have the truncated *Mertk* gene found in *mer*^{kd} mice, and not the null mutation found in RCS rats, to examine potential differences in mechanisms of degeneration between the two types of mutations in the same species.

Alternatively, the mechanism of degeneration may be similar between RCS rats and *mer*^{kd} mice, but the acute effect of SES is different in these models. In this scenario, it is possible that the current generated by the implant in response to ambient light and weekly ERG flashes was insufficient to provoke a neuroprotective response from the retina in the *mer*^{kd} mice. Further studies would be needed to show whether the lack of neuroprotection in these mice resulted from an ineffective dose of SES. However, it should be noted that similarly increased expression in FGF2 ($\sim$6.5$\times$) was measured in both the RCS rats[37] and the *mer*^{kd} mice described here after SES, suggesting that the dose of SES used here was sufficient for growth factor upregulation.

Another possibility for the difference in effect of SES on RCS rats and *mer*^{kd} mice is that mice and rats are not as similar as commonly thought. One study showed that laser photocoagulation therapy causes preservation of photoreceptors in RCS rats but not in rds mice.[68] Mounting evidence shows that mice and rats have different reactions to growth factors. One study using RAAV.CNTF treatments in rds mice and S334-ter and P23H transgenic rats showed no effect on retinal function in mice but a marked decrease in function for rats.[69] In our studies, both RCS rats and *mer*^{kd} mice showed an elevation in *Fgf2* growth factor expression 9 days after surgery.[37] This upregulation, however, was associated only with neuroprotection in the RCS rats. Further supporting species differences in responsivity to growth factors is a study by LaVail et al.[70] of neuroprotection in albino mice and rats after light damage. Similar to the differences we have noted between mice and rats treated with SES, his study found that *bFGF* (i.e., *Fgf2*) showed significant preservation of photoreceptors in rats but not in mice. The differences in response to *Fgf2* upregulation in these two species could be attributed to differences in the availability and location of Fgf2 receptors. Given these differences in similar animal model reactions to similar treatments, it is prudent to use caution when testing therapies in only one animal model.

References

1. Bressler NM, Silva JC, Bressler SB, Fine SL, Green WR. Clinicopathologic correlation of drusen and retinal pigment epithelial abnormalities in age-related macular degeneration. *Retina.* 1994;14: 130–142.
2. Green WR. Histopathology of age-related macular degeneration. *Mol Vis.* 1999;5:27.
3. Ma W, Zhao L, Fontainhas AM, Fariss RN, Wong WT. Microglia in the mouse retina alter the structure and function of retinal pigmented epithelial cells: a potential cellular interaction relevant to AMD. *PLoS One.* 2009;4:e7945.
4. Wong TY, Chakravarthy U, Klein R, et al. The natural history and prognosis of neovascular age-related macular degeneration: a systematic review of the literature and meta-analysis. *Ophthalmology.* 2008;115:116–126.
5. Young RW. Pathophysiology of age-related macular degeneration. *Surv Ophthalmol.* 1987;31:291–306.
6. Zarbin MA. Current concepts in the pathogenesis of age-related macular degeneration. *Arch Ophthalmol.* 2004;122:598–614.
7. Gal A, Li Y, Thompson DA, et al. Mutations in MERTK, the human orthologue of the RCS rat retinal dystrophy gene, cause retinitis pigmentosa. *Nat Genet.* 2000;26:270–271.
8. Feng W, Yasumura D, Matthes MT, LaVail MM, Vollrath D. Mertk triggers uptake of photoreceptor outer segments during phagocytosis by cultured retinal pigment epithelial cells. *J Biol Chem.* 2002;277:17016–17022.
9. Herron WL, Riegel BW, Myers OE, Rubin ML. Retinal dystrophy in the rat—a pigment epithelial disease. *Invest Ophthalmol.* 1969;8: 595–604.
10. Bok D, Hall MO. The role of the pigment epithelium in the etiology of inherited retinal dystrophy in the rat. *J Cell Biol.* 1971;49:664–682.
11. Dowling JE, Sidman RL. Inherited retinal dystrophy in the rat. *J Cell Biol.* 1962;14:73–109.
12. LaVail MM, Battelle BA. Influence of eye pigmentation and light deprivation on inherited retinal dystrophy in the rat. *Exp Eye Res.* 1975;21:167–192.
13. Duncan JL, LaVail MM, Yasumura D, et al. An RCS-like retinal dystrophy phenotype in mer knockout mice. *Invest Ophthalmol Vis Sci.* 2003;44:826–838.
14. Strauss O, Stumpff F, Mergler S, Wienrich M, Wiederholt M. The Royal College of Surgeons rat: an animal model for inherited retinal degeneration with a still unknown genetic defect. *Acta Anat (Basel).* 1998;162:101–111.
15. LaVail MM. Legacy of the RCS rat: impact of a seminal study on retinal cell biology and retinal degenerative diseases. *Prog Brain Res.* 2001;131:617–627.
16. D'Cruz PM, Yasumura D, Weir J, et al. Mutation of the receptor tyrosine kinase gene Mertk in the retinal dystrophic RCS rat. *Hum Mol Genet.* 2000;9:645–651.
17. Camenisch TD, Koller BH, Earp HS, Matsushima GK. A novel receptor tyrosine kinase, Mer, inhibits TNF-alpha production and lipopolysaccharide-induced endotoxic shock. *J Immunol.* 1999; 162:3498–3503.
18. Peng YW, Senda T, Hao Y, Matsuno K, Wong F. Ectopic synaptogenesis during retinal degeneration in the royal college of surgeons rat. *Neuroscience.* 2003;119:813–820.
19. Acland GM, Aguirre GD, Ray J, et al. Gene therapy restores vision in a canine model of childhood blindness. *Nat Genet.* 2001;28:92–95.
20. Bennett J, Tanabe T, Sun D, et al. Photoreceptor cell rescue in retinal degeneration (rd) mice by in vivo gene therapy. *Nat Med.* 1996;2:649–654.
21. LaVail MM, Yasumura D, Matthes MT, et al. Ribozyme rescue of photoreceptor cells in P23H transgenic rats: long-term survival and late-stage therapy. *Proc Natl Acad Sci U S A.* 2000;97:11488–11493.
22. Faktorovich EG, Steinberg RH, Yasumura D, Matthes MT, LaVail MM. Photoreceptor degeneration in inherited retinal dystrophy delayed by basic fibroblast growth factor. *Nature.* 1990;347:83–86.
23. LaVail MM, Unoki K, Yasumura D, Matthes MT, Yancopoulos GD, Steinberg RH. Multiple growth factors, cytokines, and neurotrophins rescue photoreceptors from the damaging effects of constant light. *Proc Natl Acad Sci U S A.* 1992;89:11249–11253.
24. Aramant RB, Seiler MJ. Transplanted sheets of human retina and retinal pigment epithelium develop normally in nude rats. *Exp Eye Res.* 2002;75:115–125.
25. Lund RD, Ono SJ, Keegan DJ, Lawrence JM. Retinal transplantation: progress and problems in clinical application. *J Leukoc Biol.* 2003; 74:151–160.
26. Margalit E, Maia M, Weiland JD, et al. Retinal prosthesis for the blind. *Surv Ophthalmol.* 2002;47:335–356.
27. Peachey NS, Chow AY. Subretinal implantation of semiconductor-based photodiodes: progress and challenges. *J Rehabil Res Dev.* 1999;36:371–376.

28. Rizzo JF 3rd, Wyatt J, Humayun M, et al. Retinal prosthesis: an encouraging first decade with major challenges ahead. *Ophthalmology.* 2001;108:13–14.
29. Zrenner E. The subretinal implant: can microphotodiode arrays replace degenerated retinal photoreceptors to restore vision? *Ophthalmologica.* 2002;216(suppl 1):8–20; discussion 22–23.
30. Pardue MT, Phillips MJ, Yin H, et al. Neuroprotective effect of subretinal implants in the RCS rat. *Invest Ophthalmol Vis Sci.* 2005;46:674–682.
31. Morimoto T, Fujikado T, Choi JS, et al. Transcorneal electrical stimulation promotes the survival of photoreceptors and preserves retinal function in Royal College of Surgeons rats. *Invest Ophthalmol Vis Sci.* 2007;48:4725–4732.
32. Morimoto T, Fukui T, Matsushita K, et al. Evaluation of residual retinal function by pupillary constrictions and phosphenes using transcorneal electrical stimulation in patients with retinal degeneration. *Graefes Arch Clin Exp Ophthalmol.* 2006;244:1283–1292.
33. Inomata K, Shinoda K, Ohde H, et al. Transcorneal electrical stimulation of retina to treat longstanding retinal artery occlusion. *Graefes Arch Clin Exp Ophthalmol.* 2007;245:1773–1780.
34. Fujikado T, Morimoto T, Matsushita K, Shimojo H, Okawa Y, Tano Y. Effect of transcorneal electrical stimulation in patients with nonarteritic ischemic optic neuropathy or traumatic optic neuropathy. *Jpn J Ophthalmol.* 2006;50:266–273.
35. Morimoto T, Miyoshi T, Sawai H, Fujikado T. Optimal parameters of transcorneal electrical stimulation (TES) to be neuroprotective of axotomized RGCs in adult rats. *Exp Eye Res*. 2010;90:285–291.
36. Morimoto T, Miyoshi T, Matsuda S, Tano Y, Fujikado T, Fukuda Y. Transcorneal electrical stimulation rescues axotomized retinal ganglion cells by activating endogenous retinal IGF-1 system. *Invest Ophthalmol Vis Sci.* 2005;46:2147–2155.
37. Ciavatta VT, Kim M, Wong P, et al. Retinal expression of Fgf2 in RCS rats with subretinal microphotodiode array. *Invest Ophthalmol Vis Sci.* 2009;50:4523–4530.
38. Chow AY, Pardue MT, Perlman JI, et al. Subretinal implantation of semiconductor-based photodiodes: durability of novel implant designs. *J Rehabil Res Dev.* 2002;39:313–321.
39. Chow AY, Pardue MT, Chow VY, et al. Implantation of silicon chip microphotodiode arrays into the cat subretinal space. *IEEE Trans Neural Syst Rehabil Eng.* 2001;9:86–95.
40. Pardue MT, Walker TA, Faulkner AE, Kim MK, Bonner CM, McLean GY. Implantation of mouse eyes with a subretinal microphotodiode array. *Adv Exp Med Biol.* 2008;613:377–382.
41. Sagdullaev BT, DeMarco PJ, McCall MA. Improved contact lens electrode for corneal ERG recordings in mice. *Doc Ophthalmol.* 2004;108:181–184.
42. Peachey NS, Alexander KR, Fishman GA. The luminance-response function of the dark-adapted human electroretinogram. *Vision Res.* 1989;29:263–270.
43. Pugh EN Jr, Falsini B, Lyubarsky AL. *The Origins of the Major Rod- and Cone- Driven Components of the Rodent Electroretinogram and the Effect of Age and Light-Rearing History of the Magnitude of These Components*. New York: Plenum Press; 1998.
44. Robson JG, Frishman LJ. Response linearity and kinetics of the cat retina: the bipolar cell component of the dark-adapted electroretinogram. *Vis Neurosci.* 1995;12:837–850.
45. Wurziger K, Lichtenberger T, Hanitzsch R. ON-bipolar cells and depolarising third-order neurons as the origin of the ERG-b-wave in the RCS rat. *Vision Res.* 2001;41:1091–1101.
46. Lei B, Yao G, Zhang K, Hofeldt KJ, Chang B. Study of rod- and cone-driven oscillatory potentials in mice. *Invest Ophthalmol Vis Sci.* 2006;47:2732–2738.
47. Liu K, Akula JD, Hansen RM, Moskowitz A, Kleinman MS, Fulton AB. Development of the electroretinographic oscillatory potentials in normal and ROP rats. *Invest Ophthalmol Vis Sci.* 2006;47:5447–5452.
48. Akula JD, Mocko JA, Moskowitz A, Hansen RM, Fulton AB. The oscillatory potentials of the dark-adapted electroretinogram in retinopathy of prematurity. *Invest Ophthalmol Vis Sci.* 2007;48:5788–5797.
49. Bui BV, Armitage JA, Vingrys AJ. Extraction and modelling of oscillatory potentials. *Doc Ophthalmol.* 2002;104:17–36.
50. Rozen S, Skaletsky H. Primer3 on the WWW for general users and for biologist programmers. *Methods Mol Biol.* 2000;132:365–386.
51. Yonemura D, Aoki T, Tsuzuki K. Electroretinogram in diabetic retinopathy. *Arch Ophthalmol.* 1962;68:19–24.
52. Holopigian K, Greenstein VC, Seiple W, Hood DC, Ritch R. Electrophysiologic assessment of photoreceptor function in patients with primary open-angle glaucoma. *J Glaucoma.* 2000;9:163–168.
53. Pinilla I, Lund RD, Sauve Y. Contribution of rod and cone pathways to the dark-adapted electroretinogram (ERG) b-wave following retinal degeneration in RCS rats. *Vision Res.* 2004;44:2467–2474.
54. Machida S, Chaudhry P, Shinohara T, et al. Lens epithelium-derived growth factor promotes photoreceptor survival in light-damaged and RCS rats. *Invest Ophthalmol Vis Sci.* 2001;42:1087–1095.
55. Frishman LJ, Sieving PA. Evidence for two sites of adaptation affecting the dark-adapted ERG of cats and primates. *Vision Res.* 1995;35:435–442.
56. Brown KT. The electroretinogram: its components and their origins. *UCLA Forum Med Sci.* 1969;8:319–378.
57. Ogden TE. The oscillatory waves of the primate electroretinogram. *Vision Res.* 1973;13:1059–1074.
58. Rangaswamy NV, Hood DC, Frishman LJ. Regional variations in local contributions to the primate photopic flash ERG: revealed using the slow-sequence mfERG. *Invest Ophthalmol Vis Sci.* 2003;44:3233–3247.
59. Moller A, Eysteinsson T. Modulation of the components of the rat dark-adapted electroretinogram by the three subtypes of GABA receptors. *Vis Neurosci.* 2003;20:535–542.
60. Dong CJ, Agey P, Hare WA. Origins of the electroretinogram oscillatory potentials in the rabbit retina. *Vis Neurosci.* 2004;21:533–543.
61. La Vail MM. Survival of some photoreceptor cells in albino rats following long-term exposure to continuous light. *Invest Ophthalmol.* 1976;15:64–70.
62. Pardue MT, Phillips MJ, Yin H, et al. Possible sources of neuroprotection following subretinal silicon chip implantation in RCS rats. *J Neural Eng.* 2005;2:S39–S47.
63. Woch G, Aramant RB, Seiler MJ, Sagdullaev BT, McCall MA. Retinal transplants restore visually evoked responses in rats with photoreceptor degeneration. *Invest Ophthalmol Vis Sci.* 2001;42:1669–1676.
64. Sagdullaev BT, Aramant RB, Seiler MJ, Woch G, McCall MA. Retinal transplantation-induced recovery of retinotectal visual function in a rodent model of retinitis pigmentosa. *Invest Ophthalmol Vis Sci.* 2003;44:1686–1695.
65. Nir I, Harrison JM, Liu C, Wen R. Extended photoreceptor viability by light stress in the RCS rats but not in the opsin P23H mutant rats. *Invest Ophthalmol Vis Sci.* 2001;42:842–849.
66. Ball SL, Pardue MT, Chow AY, Chow VY, Peachey NS. Subretinal implantation of photodiodes in rodent models of photoreceptor degeneration. In: Hollyfield JG, Anderson RE, LaVail MM, eds. *IX International Symposium on Retinal Degeneration*. New York: Kluwer/Plenum Press; 2001:175–180.
67. Pardue MT, Stubbs EB Jr, Perlman JI, Narfstrom K, Chow AY, Peachey NS. Immunohistochemical studies of the retina following long-term implantation with subretinal microphotodiode arrays. *Exp Eye Res.* 2001;73:333–343.
68. Xiao M, Sastry SM, Li ZY, et al. Effects of retinal laser photocoagulation on photoreceptor basic fibroblast growth factor and survival. *Invest Ophthalmol Vis Sci.* 1998;39:618–630.
69. Liang FQ, Aleman TS, Dejneka NS, et al. Long-term protection of retinal structure but not function using RAAV.CNTF in animal models of retinitis pigmentosa. *Mol Ther.* 2001;4:461–472.
70. LaVail MM, Yasumura D, Matthes MT, et al. Protection of mouse photoreceptors by survival factors in retinal degenerations. *Invest Ophthalmol Vis Sci.* 1998;39:592–602.
71. Weymouth AE, Vingrys AJ. Rodent electroretinography: methods for extraction and interpretation of rod and cone responses. *Prog Retin Eye Res.* 2008;27:1–44.
72. Peachey NS, Goto Y, al-Ubaidi MR, Naash MI. Properties of the mouse cone-mediated electroretinogram during light adaptation. *Neurosci Lett.* 1993;162:9–11.